

## **THEORETICAL ANALYSIS OF STRESS DISTRIBUTIONS IN FRP SIDE-BONDED TO RC BEAMS FOR SHEAR STRENGTHENING**

X. Z. Lu<sup>1</sup>, J. F. Chen<sup>2</sup>, L. P. Ye<sup>1</sup>, J. G. Teng<sup>3</sup> and J. M. Rotter<sup>2</sup>

<sup>1</sup> Department of Civil Engineering, Tsinghua University, Beijing, China  
Email: luxinzheng@263.net, ylp@mail.tsinghua.edu.cn

<sup>2</sup> Institute for Infrastructure and Environment, Edinburgh University  
The King's Buildings, Edinburgh EH9 3JF, UK  
Email: j.f.chen@ed.ac.uk, m.rotter@ed.ac.uk

<sup>3</sup> Department of Civil and Structural Engineering, The Hong Kong Polytechnic University, Hong Kong, China  
Email: cejgteng@polyu.edu.hk

### **ABSTRACT**

Extensive research has been conducted on the strengthening of reinforced concrete (RC) beams with externally bonded fibre reinforced polymer (FRP) composites in the last decade. The FRP composites are usually installed following one of three common schemes: complete wrapping, U jacketing, and side bonding (bonding on their sides only). Experimental studies have shown that most side-bonded beams fail due to debonding of the FRP from the concrete. A key factor influencing the contribution of the FRP to the shear capacity of the beam is the stress (or strain) distribution in the FRP at the ultimate limit state. This paper presents a theoretical study of the stress distribution in the FRP along the critical shear crack at debonding failure of side-bonded beams for several assumed crack width variations, using a rigorous FRP-to-concrete bond-slip model. Numerical results show that Chen and Teng's (2001a, 2003a) simple assumption for the stress distribution in the FRP results in satisfactory predictions for the effective FRP stress in most cases. However, it can become unconservative for beams lightly reinforced in flexure but this is less relevant in practice because flexure rather than shear is the intended control failure mode.

### **KEYWORDS**

FRP, RC beams, strengthening, interfacial stresses, shear strength.

### **INTRODUCTION**

Extensive research has been conducted on the strengthening of reinforced concrete (RC) beams with externally bonded fibre reinforced polymer (FRP) composites (ACI 2002, Chaallal *et al.* 1998, Chen and Teng 2001a, b, Chen and Teng 2003a, b, Concrete Society 2004, fib 2001, ISIS 2001, JSCE 2000, Khalifa *et al.* 1998, Maeda *et al.* 1998, Taljsten 2003, Teng *et al.* 2002, 2003, Triantafillou 1998). RC beams can be shear-strengthened through complete wrapping, U jacketing or side bonding (bonding of FRP on the beam sides only). The main shear failure modes of shear-strengthened RC beams are FRP rupture and debonding (Teng *et al.* 2002, 2003). In both failure modes, the stress (or strain) distribution in the FRP at the ultimate limit state is non-uniform and is a key factor influencing the contribution of the FRP to the shear capacity of the beam for all three strengthening schemes (Chen and Teng 2003a,b). Based on a number of simple but rational assumptions, Chen and Teng (2003a,b) proposed methods for predicting the maximum values of the FRP stress and the stress distribution factors for both failure modes.

Experimental research shows that most side-bonded beams fail due to debonding of the FRP from the concrete. This paper presents a simple theoretical study on the stress distribution in the FRP along the critical shear crack at debonding failure in side-bonded beams. A recently developed FRP-to-concrete bond-slip model (Lu *et al.* 2005a) was used in this study. Several idealised crack width variations, which are closely related to the FRP slip field along the critical shear crack, are investigated. The results are compared with Chen and Teng's (2003a) simple predictive model. For convenience of description, the bonded FRP reinforcement is assumed to be in the form of strips, with a continuous sheet being a special case or a smeared equivalent representation of strips. Depending on the context, either "strips" or "sheets" may be used to refer to the bonded FRP reinforcement.

## EXISTING SHEAR STRENGTH MODELS FOR DEBONDING FAILURES

A number of models for the shear strength of FRP-strengthened RC beams have been proposed for design use (Chaallal *et al.* 1998, Khalifa *et al.* 1998, Triantafillou 1998, Taljsten 2003, Chen and Teng 2003a,b). In most of these proposals, the shear strength of an FRP-strengthened RC beam  $V_n$  is evaluated by assuming that the contributions of the concrete  $V_c$ , the steel shear reinforcement  $V_s$ , and the bonded FRP reinforcement  $V_f$  are additive, i.e.

$$V_n = V_c + V_s + V_f \quad (1)$$

Because it is usually proposed that  $V_c$  and  $V_s$  should be calculated according to provisions in existing design codes, the main differences between the available proposals lie in the evaluation of the FRP contribution  $V_f$ .

Steel stirrups have a small elastic strain limit but excellent ductility, so all stirrups intersected by the critical shear crack can reach their yield stress at the shear failure of the RC beam as a result of stress re-distribution. This means that their yield strength is fully utilized and the stress distribution in the steel stirrups along the critical shear crack is uniform. By contrast, both FRP rupture and debonding failures are brittle processes that allow little or limited stress redistribution, so the stress distribution in the FRP along the shear crack at the ultimate limit state is non-uniform and can significantly affect the FRP contribution to the shear capacity of the beam.

Chen and Teng (2001a,b) were probably the first to propose the explicit inclusion of the effect of non-uniform stress distribution in the FRP on the shear capacity. The FRP contribution in their model (Chen and Teng 2003a,b) is given by:

$$V_f = 2f_{fe}t_f w_f \frac{h_{fe}(\cot \theta + \cot \beta) \sin \beta}{s_f} \quad (2)$$

where  $\theta$  is the critical shear crack angle,  $\beta$  the angle between the fibre and beam longitudinal axis,  $h_{fe}$  is the effective height of the FRP,  $w_f$  is the width of the FRP strip,  $s_f$  is the centre to centre spacing of FRP strips along the beam longitudinal axis, and the effective FRP stress  $f_{fe}$  is defined as the maximum FRP stress  $\sigma_{f,max}$  times the stress distribution factor  $D_f$

$$f_{fe} = D_f \sigma_{f,max} \quad (3)$$

For debonding failures, the maximum FRP stress  $\sigma_{f,max}$  is calculated according to Chen and Teng's bond strength model (2001c), which is given as:

$$\sigma_{f,max} = \min \left\{ \begin{array}{l} f_{fu} \\ 0.427 \beta_L \beta_w \sqrt{\frac{E_f \sqrt{f_c'}}{t_f}} \end{array} \right., \quad \beta_L = \begin{cases} 1 & \text{if } \lambda \geq 1 \\ \sin \frac{\pi \lambda}{2} & \text{if } \lambda < 1 \end{cases}, \quad \lambda = \frac{L_{max}}{L_e} \quad (4a,b,c)$$

$$L_{max} = \begin{cases} \frac{h_{fe}}{\sin \beta} & \text{for U-jackets} \\ \frac{h_{fe}}{2 \sin \beta} & \text{for side plates} \end{cases}, \quad L_e = \sqrt{\frac{E_f t_f}{\sqrt{f_c'}}}, \quad \beta_w = \sqrt{\frac{2 - w_f / (s_f \sin \beta)}{1 + w_f / (s_f \sin \beta)}} \quad (4d,e,f)$$

in which  $f_c'$  (MPa) is the cylinder compressive strength of the concrete, and  $E_f$  (MPa) and  $f_{fu}$  (MPa) are the Young's modulus and the tensile strength of the FRP respectively.

Assuming that all bonded FRP strips intersected by the critical shear crack can develop the full bond strength at the ultimate limit state, Chen and Teng (2003a) deduced the FRP stress distribution factor as

$$D_f = \begin{cases} \frac{2}{\pi \lambda} \frac{1 - \cos \frac{\pi \lambda}{2}}{\sin \frac{\pi \lambda}{2}} & \text{if } \lambda \leq 1 \\ 1 - \frac{\pi - 2}{\pi \lambda} & \text{if } \lambda > 1 \end{cases} \quad (5)$$

Because both  $D_f$  and  $\beta_L$  are functions of the normalised maximum bond length  $\lambda$ , the following modified FRP stress factor  $D_{fL}$  is defined here for convenience of comparison with numerical results presented later:

$$D_{fL} = D_f \beta_L \quad (6)$$

Using Eq. 6, the effective FRP stress of Eq. 3 can alternatively be expressed as:

$$f_{fe} = D_f \sigma_{f \max} = D_f \beta_L \sigma_{f, \text{inf}} = D_{\beta L} \sigma_{f, \text{inf}} \quad (7)$$

where  $\sigma_{f, \text{inf}}$  is the FRP debonding stress when the FRP bond length is infinite:

$$\sigma_{f, \text{inf}} = 0.427 \beta_w \sqrt{\frac{E_f \sqrt{f_c'}}{t_f}} \quad (8)$$

Furthermore, for ease of comparison for different forms of crack width variations and for both U jacketing and side bonding, a normalised bond length at the middle of the critical shear crack  $\lambda'$  is defined here, which equals the normalised maximum bond length  $\lambda$  for side-bonding but half of that in U-jacketing as follows:

$$\lambda' = \frac{L_{\text{mid}}}{L_e} = \frac{h_{fe}}{2L_e \sin \beta} = \lambda_{\text{side-bonding}} = \frac{\lambda_{\text{U-jacketing}}}{2} \quad (9)$$

Clearly, the assumption adopted by Chen and Teng (2003a) for deriving the FRP stress distribution factor that all FRP strips intersected by the critical shear crack can reach the full bond strength at the ultimate limit state is simplistic. The aim of this study is to assess the validity of this assumption.

### IDEALISATION OF THE FRP SLIP FIELD ALONG THE CRITICAL SHEAR CRACK

Shear cracking in concrete beams is a complex phenomenon. There is still a lack of accurate methods for predicting the initiation and propagation of these cracks. Depending on many factors such as loading, amount and detailed arrangement of internal reinforcement and the properties of concrete, there may be one or more diagonal cracks. However, unless the shear failure is due to diagonal compression which often occurs in beams with a very small shear span-to-depth ratio, there is usually a critical shear crack which dominates the shear failure process. In some beams, such as those with a large shear span-to-depth ratio, the critical shear crack may be the only crack intersecting the FRP strips on the beam sides. It may be noted that the FRP-to-concrete bond resistance may be increased if there are more than one crack intersecting the FRP strip (Teng *et al.* 2005). Therefore, it is conservatively assumed in this study that secondary shear cracks are insignificant compared with the critical shear crack intersecting the FRP strips in determining the interfacial behaviour between the FRP strip and the concrete substrate.

Provided that the critical shear crack is predominant over other shear cracks, the interfacial slips (and thus stresses) between an FRP strip and the substrate concrete are then almost wholly induced by the widening of this crack. Clearly, the sum of the interfacial slips on both sides of the critical shear crack equals the crack width. This means that the bond-slip behaviour of the FRP-to-concrete interface is predominately controlled by the width of the critical shear crack at the location where it intersects the FRP strip, and that the variation of this width determines the stress distribution in the FRP along the critical shear crack.

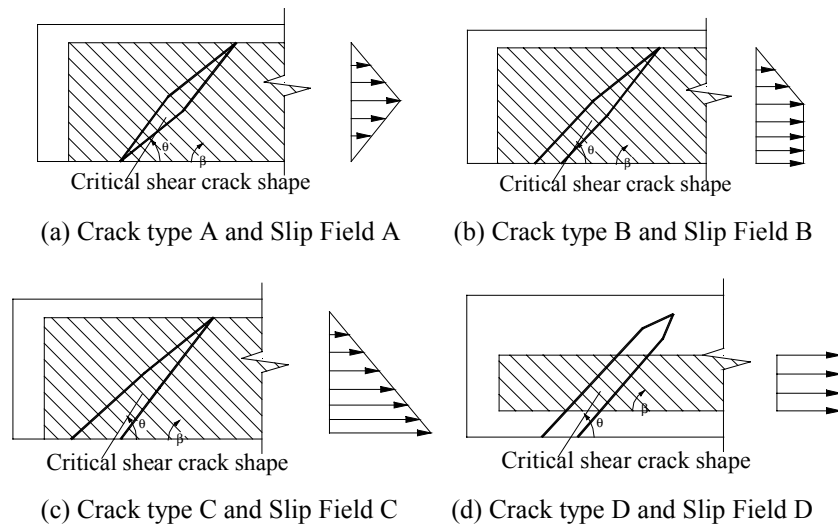


Figure 1 Typical idealised crack shapes and slip fields

Because of the lack of information on the precise shape of the critical shear crack, four simple crack types as shown in Figure 1 are considered in this study. Note that the shape of the critical shear crack may be close to Type A (Figure 1a) in beams very heavily reinforced in flexure. The critical shear crack may be expected to be closer to Type C (Figure 1c) in beams with minimal flexural reinforcement but this may have less relevance in practice because flexural failure is likely to be the control failure mode for such beams. The crack shape for most practical beams is likely to lie between these two cases and may be close to Type B (Figure 1b). If the FRP strips cover only part of the beam height, it is possible that the critical shear crack is fairly uniform within the effective FRP height (Figure 1d). It is further assumed here that the slips between FRP and concrete on the two sides of the critical shear crack are symmetrical. This means that the distribution of slip along the critical shear crack is assumed to follow the shape of the crack. The FRP slip fields corresponding to the four crack shapes are termed here as Slip Fields A~D respectively (Figure 1).

## COMPUTATIONAL MODELS

In side-bonded beams considered in this study, the critical shear crack divides each FRP strip into two parts and it is reasonable to assume that the shorter part will fail by debonding, as shown in Figure 2. Those FRP strips likely to debond at failure are marked as the “critical FRP” in Figure 2. In the finite element analysis described below, only the bond resistance of this critical FRP area was considered. Based on the assumption that the interfacial slips on the two sides of the critical shear crack are symmetrical, the interfacial slip of the FRP in the critical area above the crack equals half of the width of the critical shear crack. As a result, four simplified computational models (Figure 2) can be established, corresponding to the four types of cracks (Figure 1). It may be noted that the assumption that the slip is symmetrical on the two sides of the crack is not exactly valid, but numerical results from more complete models considering the full height of the FRP intersected by the crack show that the error resulting from this simplified treatment is insignificant.

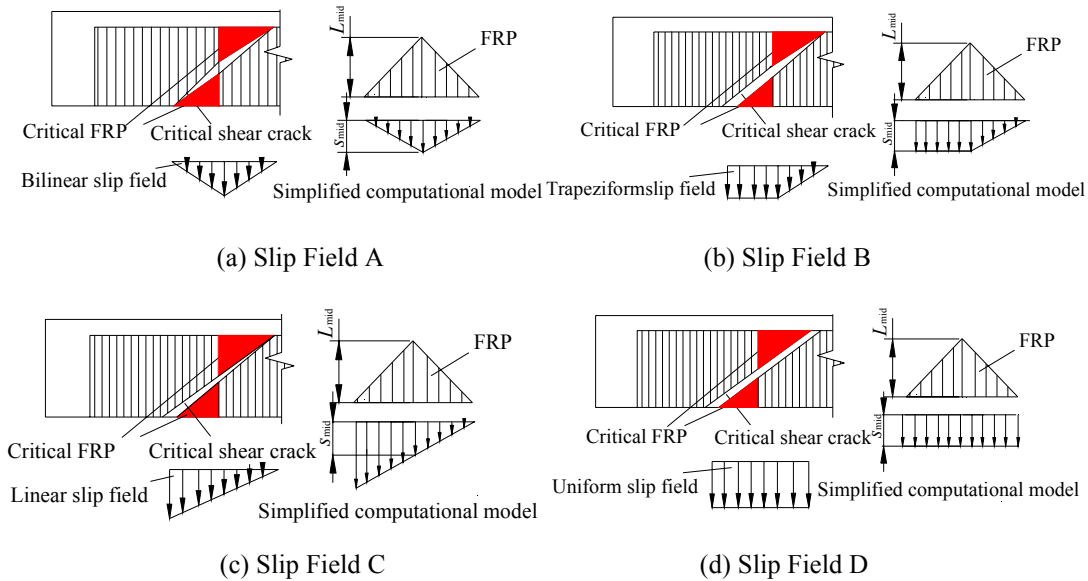


Figure 2 Computational models

## Finite element implementation

The idealised computational models shown in Figure 2 were implemented using ANSYS (1999). The FRP strips were modelled by a series of truss elements, whilst the interfaces were modelled by a series of spring elements, as shown in Figure 3. The truss elements were connected to the rigid substrate concrete (e.g. deformations of un-cracked concrete were ignored) using the spring elements. The bond-slip relationship proposed by Lu et al. (2005a) (Figure 4) was used to derive the properties of the spring elements. The LINK 1 element in ANSYS was used to model the FRP truss elements and the COMBIN 39 element was used to model the spring elements.

The development of the debonding process was simulated by imposing an increasing boundary displacement corresponding to the considered slip field on the truss nodes along the critical shear crack. An analysis was terminated when the average stress in the FRP  $\sigma_{f,ave}$  was reduced to half of its peak value. The results were then used to deduce the average FRP stress and the FRP stress distribution factor at different slip values.

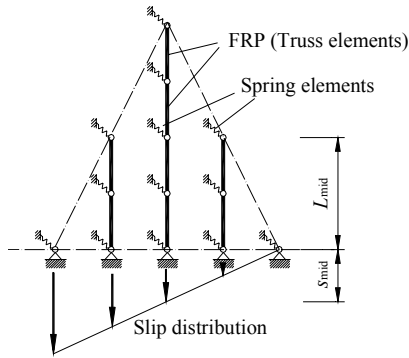


Figure 3 Finite element models (Slip Field C)

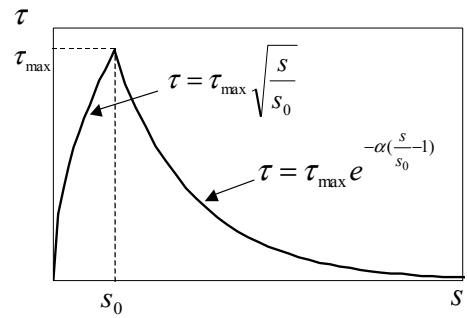


Figure 4 Bond-slip model (Lu *et al.* 2005a)

## NUMERICAL RESULTS

### Development of stresses in FRP

Figure 5 shows a typical example of the variation of the average FRP stress against the increase of slip at the mid-height of the effective FRP for a side-bonded beam for the four different slip fields. Here the average FRP stress  $\sigma_{f,ave}$  is normalised by  $\sigma_{f,inf}$ , and the slip at the mid-height  $s_{mid}$  is normalised by the slip at the peak interfacial stress  $s_0$  (Figure 4). The same parameters adopted in a previous study on U jacketed beams (Lu *et al.* 2005b) were used here: concrete tensile strength  $f_t = 3\text{MPa}$ , axial stiffness of FRP  $E_{tf} = 16\text{GPa}\cdot\text{mm}$ , FRP strip width to spacing ratio  $w_f/s_f = 0.5$ , normalised FRP bond length at the mid-length of the crack (or mid-crack)  $\lambda' = 1.5$ .

In slip field A, the average FRP stress  $\sigma_{f,ave}$  increases smoothly and reaches its peak value when the normalised slip at the mid-height of the beam is about 4.2 (corresponding to a maximum crack width of about 0.49mm for Models A, B and D but 0.98mm for Model C for the concrete properties adopted above). The peak average FRP stress is the largest among the four slip fields considered because the critical FRP area matches the geometry of the slip field so that the bond strengths of almost all the FRP strips are reached simultaneously. However, this also means that all FRP strips are separated from the concrete almost at the same time, leading to an abrupt descending branch on the slip versus FRP stress curve and a very brittle failure (Figure 5).

Among the four slip models, slip field C produces the smallest FRP average stress  $\sigma_{f,ave}$ . This is because the bond length of the FRP strip at the bottom of the critical shear crack is very small whilst the slip is largest there and decreases linearly to zero at the top for slip field C, leading to progressive debonding of FRP strips starting from the bottom of the crack shortly after the critical shear crack appears. However, this progressive failure process of FRP strips also means a significant plateau on the FRP stress-slip curve, resulting in the greatest ductility among the four slip fields (Figure 5). Both the peak FRP average stress and the ductility from slip field B are clearly between those from slip fields A and C.

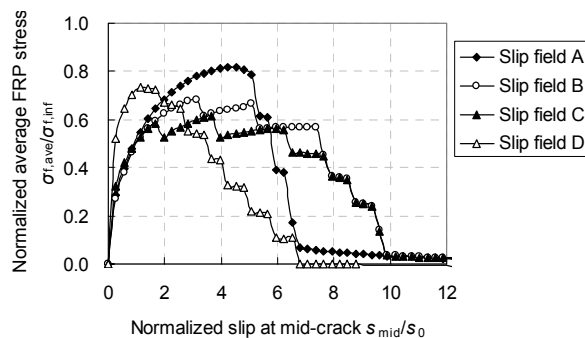


Figure 5 Variation of average FRP stress with slip

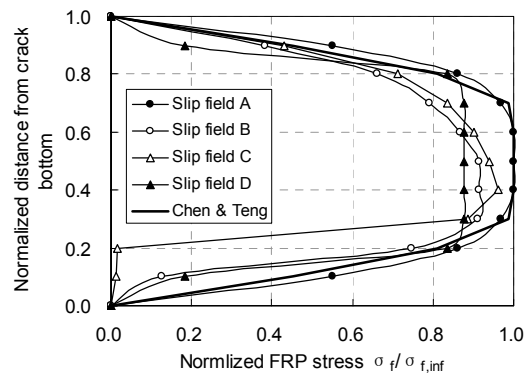


Figure 6 FRP stress distribution at peak average stress ( $\lambda' = 1.5$ )

The peak FRP average stress in slip field D is reached at a much smaller slip value compared with the other three slip fields because all the FRP strips are subjected to the same slip so that the FRP strips at both the top and bottom first reach their bond strengths simultaneously in this case whilst only the bottom strip (in slip field B and C) or middle strip (in slip field A) first reaches the bond strength.

Figure 6 shows the FRP stress distributions at their corresponding peaks of the FRP average stress predicted from the four models with  $\lambda' = 1.5$ . The distribution predicted by Chen and Teng's model (2001a, 2003a) is also shown for comparison. It is seen that Chen and Teng's prediction is in very close agreement with that of slip field A but overestimates those of other slip fields due to early debonding failure of FRP at the bottom of the shear crack. The implications of this observation for practical situations are discussed later.

### Effect of beam size on FRP stress distribution

If the FRP strips are bonded to the full height of the beam on both sides, the normalised FRP bond length  $\lambda'$  is proportional to the beam height. Therefore, the effect of the beam size on the FRP stress distribution can be investigated by varying the normalised FRP bond length  $\lambda'$ . For different  $\lambda'$  values, Figure 7 shows the FRP stress distributions corresponding to the peak FRP average stress for Model A. The FRP stress distribution is close to the shape of the slip field (bilinear in Model A) when  $\lambda'$  is very small because the slip is the largest at the middle where the FRP bond length is also the largest. As the normalised bond length increases, the maximum FRP stress also increases until the maximum bond length (at the middle of the crack) reaches the effective bond length. After that, the stress distribution in the FRP becomes more and more uniform because the FRP stress cannot exceed  $\sigma_{f,inf}$ .

### Relationship between $D_{fl}$ and $\lambda'$

Equation 7 shows that the effective FRP stress can be easily obtained if the modified FRP stress factor  $D_{fl}$  is given. Furthermore, the FRP contribution to the shear capacity is proportional to  $D_{fl}$ . The effect of the bond length (beam size) on  $D_{fl}$  is investigated here for the four slip fields (Figure 8). Chen and Teng's (2001a, 2003a) prediction is also shown for comparison. Although the four crack shapes are significantly different and they may represent some extreme scenarios, the predicted FRP stress factors are not significantly different. The maximum difference between the four models for  $\lambda'=2$  is about 20%. Chen and Teng's predictions lie between these four curves: they are slightly lower than the predictions from Model A and slightly higher than those from Models B and D (about 5% on both side when  $\lambda'=2$ ). However, the difference can be significant (~15%) if the crack shape is close to Model C and Chen and Teng's model is on the unconservative side. As noted earlier, the latter would only occur in beams reinforced with light flexural reinforcement, in which case shear failure is unlikely to be the critical failure mode.

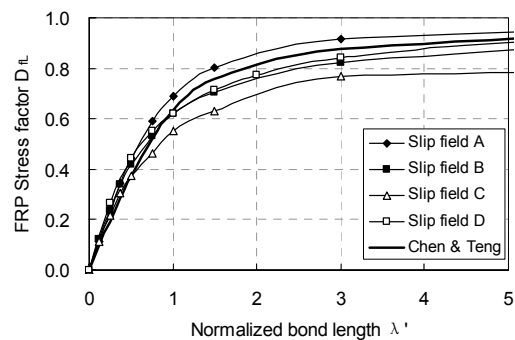
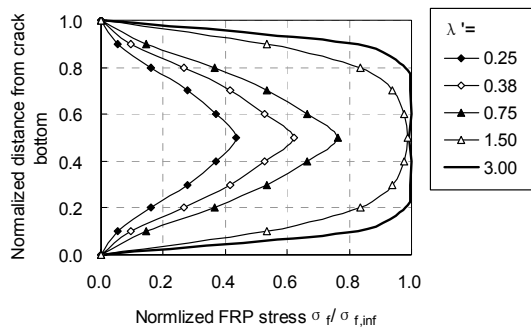


Figure 7 FRP stress distributions at peak average stress (Slip Field A) Figure 8  $D_{fl} \sim \lambda'$  relationship from different slip models

## CONCLUSIONS

This paper has presented a theoretical study on stress distributions in FRP strips/sheets bonded to the sides of RC beams for enhanced shear resistance when shear failure of the beam occurs by the debonding of the FRP from the concrete. Four different idealised crack shapes for the critical shear crack were considered. A rigorous FRP-to-concrete bond-slip model was used to represent the interfacial behaviour between the FRP and the concrete substrate. The finite element method was employed to model the behaviour of an idealised system consisting of FRP strips bonded to rigid concrete prisms. Although the different critical shear crack models result in significantly different stress distributions in the FRP, their effect on the stress distribution factor is much less

significant. The study shows that Chen and Teng's (2001a, 2003a) simple assumption for the stress distribution in the FRP results in satisfactory predictions in most cases for the effective FRP stress but it may be unconservative for beams with light flexural reinforcement.

## ACKNOWLEDGMENTS

The authors would like to acknowledge the financial support provided by the Royal Society through the Royal Society-NSFC UK-China Joint Project (Grant No. IS 16657), the Research Grants Council of the Hong Kong Special Administrative Region, China (Project No: PolyU 5151/03E), and the National Natural Science Foundation of China through a key project for FRP in construction (Project No. 50238030).

## REFERENCES

- ACI (2002). *Guide for the Design and Construction of Externally Bonded FRP Systems for Strengthening Concrete Structures*, ACI 440.2R-02, American Concrete Institute.
- ANSYS. (1999). *User's Manual*, ANSYS Company.
- Chen, J.F. and Teng, J.G. (2001a). "Shear strengthening of RC beams by external bonding of FRP composites: a new model for FRP debonding failure", *Proc., 9th International Conference on Structural Faults and Repair*, 4-6, July, London, (CD-ROM).
- Chen, J.F. and Teng, J.G. (2001b). "A shear strength model for FRP strengthened RC beams", *Proc., 5th International Conference on Fibre-Reinforced Plastics for Reinforced Concrete Structures (FRPRCS-5)*, Cambridge, 16-18 July, 205-214.
- Chen, J.F. and Teng, J.G. (2001c). "Anchorage strength models for FRP and steel plates bonded to concrete", *Journal of Structural Engineering*, ASCE, 127(7), 784-791.
- Chen, J.F. and Teng, J.G. (2003a). "Shear capacity of FRP-strengthened RC beams: FRP debonding", *Construction and Building Materials*, 17, 27-41.
- Chen, J.F. and Teng, J.G. (2003b). "Shear capacity of FRP strengthened RC beams: fibre reinforced polymer rupture", *Journal of Structural Engineering*, ASCE, 129(5), 615-625.
- Chaallal, O., Nollet, M. J. and Perraton, D. (1998). "Strengthening of reinforced concrete beams with externally bonded fiber-reinforced-plastic plates: design guidelines for shear and flexure", *Canadian Journal of Civil Engineering*, 25(4), 692-704.
- Concrete Society (2004). *Design Guidance for Strengthening Concrete Structures Using Fibre Composite Materials*, Technical Report No. 55, 2<sup>nd</sup> Edition, UK.
- fib (2001). *Externally Bonded FRP Reinforcement for RC Structures*, Task Group 9.3, International Federation for Structural Concrete (fib).
- ISIS (2001). *Retrofitting Concrete Structures with Fiber Reinforced Polymers*. ISIS Canada.
- JSCE (2000). *Recommendations for Upgrading of Concrete Structures with Use of Continuous Fiber Sheets*, Research Committee on Upgrading of Concrete Structures with Use of Continuous Fiber Sheets, Japanese Society of Civil Engineers.
- Khalifa, A., Gold, W. J., Nanni, A. and Aziz, A. (1998). "Contribution of externally bonded FRP to shear capacity of RC flexural members", *Journal of Composites for Construction*, ASCE, 2(4), 195-203.
- Lu, X.Z., Teng, J.G., Ye, L.P. and Jiang, J.J. (2005a). "Bond-slip models for FRP sheets/plates externally bonded to concrete", *Engineering Structures*, 27(6), 938-950.
- Lu, X.Z., Chen, J.F., Ye, L.P., Teng, J.G. and Rotter, J.M. (2005b). "Theoretical analysis of FRP stress distribution in U jacketed RC beams", *Composites in Construction – Proc., Third International Conference on Composites in Construction (CCC2005)*, Hamelin et al. (eds), July 11-13, Lyon, France, 1, 541-548.
- Maeda, T., Asano, Y., Sato, Y., Ueda, T. and Kakuta, Y. (1998). "A study on bond mechanism of carbon fiber sheet", *Proc., 3rd International Symposium on Non-Metallic (FRP) Reinforcement for Concrete Structures*, Sapporo, 279-285.
- Taljsten, B. (2003). "Strengthening concrete beams for shear with CFRP sheets", *Construction and Building Materials*, 17(1), 15-26.
- Teng, J.G., Chen, J.F., Smith, S.T. and Lam, L. (2002). *FRP-strengthened RC Structures*, John Wiley & Sons, UK.
- Teng, J.G., Chen, J.F., Smith, S.T. and Lam, L. (2003). "Behaviour and strength of FRP-strengthened RC structures: a state-of-the-art review", *Proc. of the Institution of Civil Engineers – Structures and Buildings*, 156(SB1), 51-62.
- Teng, J.G., Yuan, H. and Chen, J.F. (2005). "Theoretical model of FRP-to-concrete interfaces between two adjacent cracks", *International Journal of Solids and Structures*, in press.
- Triantafillou, T.C. (1998). "Shear strengthening of reinforced concrete beams using epoxy-bonded FRP composites", *ACI Structural Journal*, 95(2), 107-115.